

DESIGN AND IMPLEMENTATION OF THE METOP-B ORBIT POSITIONING STRATEGY

Javier Sánchez⁽¹⁾, Miguel Ángel Martín Serrano⁽²⁾, Dirk Kuijper⁽³⁾, and Isidro Muñoz⁽⁴⁾

⁽¹⁾GMV at ESA/ESOC, Robert-Bosch straÙe 5, 64293 Darmstadt, Germany

email: javier.sanchez@esa.int

phone: +496151902416

⁽²⁾SCISYS Deutschland GmbH at ESA/ESOC, Robert-Bosch straÙe 5, 64293 Darmstadt, Germany

email: miguel.angel.martin.serrano@esa.int

phone: +496151902273

⁽³⁾Logica Deutschland GmbH at ESA/ESOC, Robert-Bosch straÙe 5, 64293 Darmstadt, Germany

email: dirk.kuijper@esa.int

phone: +496151902376

⁽⁴⁾ESA/ESOC, Robert-Bosch-StraÙe 5, 64293 Darmstadt Germany

email: isidro.munoz@esa.int

phone: +496151902108

Abstract: Launched on September 17th 2012 MetOp-B is the second of a series of three spacecraft which comprise the space segment of the EUMETSAT Polar System (EPS) programme. Although the spacecraft is operated by the European Organisation for the Exploitation of Meteorological Satellites (EUMETSAT) the Launch and Early Orbit Phase (LEOP) operations are conducted by the European Space Operations Centre (ESOC). The present paper describes the study carried out by the Flight Dynamics team at ESOC, in cooperation with EUMETSAT experts, to design the positioning strategy of MetOp-B relative to MetOp-A. The objective of this work was to analyse the positioning problem for all injection cases and to provide a guideline to be followed in LEOP, which ensures the optimal transfer of operations between both control centres. In addition to this, the experience implementing the positioning strategy during LEOP is also presented in this paper.

Keywords: MetOp, LEOP operations, relative orbit positioning, sun-synchronous, Earth observation.

1. Introduction

Launched from the Baikonur Cosmodrome in Kazakhstan MetOp-B was put in orbit by a Soyuz rocket equipped with a Fregat upper stage on the 17th of September 2012. Some 69 minutes after lift-off contact with the spacecraft was made from the Kerguelen Ground Station in the Southern Indian Ocean. Separation was then confirmed.

MetOp-B is the second of a series of three spacecraft which comprise the space segment of the EUMETSAT Polar System (EPS) programme, which constitutes a joint initiative in collaboration with the United States National Oceanic and Atmospheric Administration (NOAA) for weather and climate monitoring. The first MetOp satellite, MetOp-A, launched on October 19th 2006 has successfully provided operational meteorological observations from the beginning of its mission. Now, an extension of its activities beyond the nominal 5-year lifetime will be possible due to its excellent performances, leading to an overlap with the operational life of MetOp-B. This period

of dual operations will bring a substantial increase on the wealth and quality of the data gathered by the MetOp mission.

The Flight Dynamics Orbit Determination and Control (FD OD&C) team at ESOC was in charge of preparing a manoeuvre plan to correct the spacecraft orbit as delivered by the launcher. This plan should aim at correcting the dispersion in inclination and start the phasing with respect to MetOp-A. The large amount of possible scenarios depending on the launch day, the relatively high dispersions provided in the launcher specifications and the operational limitations on the manoeuvring capabilities made the positioning of MetOp-B a challenging task. This paper presents the study carried out by the FD OD&C team at ESOC in cooperation with EUMETSAT experts to analyze the positioning problem of MetOp-B. The objectives of the study were the following:

- Evaluation of feasibility to comply with the Hand-Over (HO) conditions established by EUMETSAT under all possible injection scenarios.
- Identification of injection scenarios that would require an extension of LEOP operations.
- Design of a positioning strategy with the ultimate goal of providing a guideline to be used during LEOP.

The short duration of the LEOP operations affected in particular the OD&C team. A prompt analysis of the possible manoeuvre strategies played a fundamental role, in particular in case an extension of the LEOP was required. Hence, the study and design of the positioning strategy was carried out using analytical models in order to allow analysing a large amount of different scenarios in a swift manner during the conduction of LEOP operations. The paper includes as well a report of the injection achieved by Soyouz and the design of the final manoeuvre sequence.

2. Mission profile description

MetOp-B is controlled following the same reference ground track as MetOp-A [1] in a polar, sun-synchronous orbit, with Local Time of Descending Node (LTDN) at 9:30 and a ground track repetition cycle of 412 orbits in 29 days. Having both spacecraft in orbit the points on the common ground track shall be revisited in either 12 or 17 days. This last condition allows two possible in-orbit positions for MetOp-B with respect to MetOp-A, which can be translated into a timing offset of ± 48.932 minutes or, equivalently, ± 173.793 degrees in PSO¹ difference.

The orbit control strategy foreseen for MetOp-B during routine operations is analogous to the one implemented for its predecessor. The perpendicular distance from the reference ground track to the sub-satellite point is kept lower than 5 km, and the Local Time is controlled within a threshold of ± 2 min around the reference.

¹ The French appellation for Argument of Latitude, Position sur l'Orbite (PSO), will be used throughout the paper, since this nomenclature is more extended within ESOC Flight Dynamics.

Table 1. MetOp-B reference orbit.

<i>Type</i>	Near Polar Sun-Synchronous
<i>LTDN</i>	09:30 h
<i>Period</i>	412 orbits in 29 days (29 days repeat ground track)
<i>Mean inclination</i>	98.7006 deg
<i>Mean semi-major axis</i>	7195.605 km
<i>Offset with respect to MetOp-A</i>	± 48.932 min ± 173.793 degrees

After lift-off the LEOP operations were conducted at ESOC, the nominal duration of this phase was 3 days. After the completion of the LEOP operations the spacecraft control was handed over to the EUMETSAT Control Centre (EUMETSAT-CC). In the nominal LEOP duration only two orbit corrections were possible, both taking place during the 3rd day of mission. Generally an Out-of-Plane (OOP) and an In-Plane (IP) manoeuvre are needed to perform respectively an inclination and a semi-major axis change. The sequence of manoeuvres had to be executed in this particular order to compensate the IP component introduced by the OOP manoeuvre. The alignment of the thrusters, which is not parallel to the velocity direction, introduces IP effects when an OOP manoeuvre is executed and vice-versa. Besides, additional non-negligible IP components are introduced due to the slews performed before and after an OOP manoeuvre. The two manoeuvring slots were scheduled at 50:18 hours and 61:22 hours from lift-off respectively. The OOP manoeuvre had to be executed in combined visibility of Kerguelen and Malindi Ground Stations (node crossing).

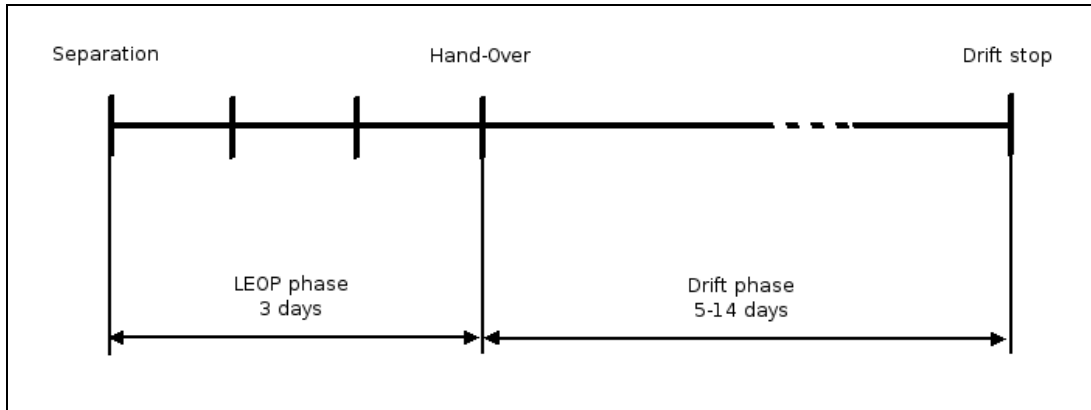


Figure 1. Depiction of the phases in early mission of MetOp-B.

After the execution of the IP manoeuvre the phasing of MetOp-B towards its final position with respect to MetOp-A is begun, starting the so-called drift phase. After the LEOP EUMETSAT-CC prepares and executes a drift-stop manoeuvre to start the first control cycle around the reference orbit.

In addition to the visibility constraint for the OOP manoeuvre, the AOCS imposed some limitations on the preparation of the manoeuvre sequence:

- The maximum size of the OOP manoeuvre was 6.8 m/s. This is equivalent to an inclination shift of 50.8 mdeg accounting for the loss of efficiency due to the manoeuvre spreading around the node crossing.
- Either a single or a double burn can be executed in the IP maneuvering slot. The same maximum size of 6.8 m/s applied to the IP burns

On top of the above mentioned maneuvering constraints underperformances of up to 4% of the delta-V size were expected.

Table 2 contains a summary of the target orbital elements at injection which were selected for MetOp-B and the STARSEM specified dispersions. The dispersion values provided in the launcher specifications were quite conservative. This point was confirmed by simulations performed by STARSEM. However, the positioning strategy had to be designed to cope with the dispersions given in Tab. 2.

Table 2. Target for STARSEM and contractual dispersions.

<i>Orbit element</i>	<i>Target with respect to the reference</i>	<i>3-sigma dispersion</i>
Semi-major axis	-16 km	±12 km
Eccentricity (e_x, e_y)	Frozen eccentricity	-
Inclination	+ 35 mdeg	±120 mdeg
LTDN	- 70 s	±26.3 s

3. Hand-Over conditions and optimization criteria

The point in time when the control of MetOp-B is transferred from ESOC to EUMETSAT-CC was defined as Hand-Over time. In order to ensure an optimal transfer of the spacecraft operations a set of HO conditions was agreed between both control centres.

- The final position of MetOp-B shall be reached between 5 and 14 days after HO. This is achieved through a set of one or several manoeuvres implemented by EUMETSAT-CC.
- No manoeuvres shall be executed during the drift phase.
- Interferences with MetOp-A shall be avoided if possible.
- The LTDN shall be kept within a dead-band of ±2 min with respect to the reference for at least 45 days after HO.

Given an arbitrary injection error on an arbitrary launch day there are different of possible positioning strategies to achieve the HO conditions. They depend on the selection of the drift parameters shown in Tab. 3.

Table 3. Possible strategies.

<i>Final position with respect to MetOp-A</i>	Target A: 173.793 deg (MetOp-B leading) Target B: -173.793 deg (MetOp-B trailing)
<i>Drift direction</i>	Forward: Drift in the flight direction (semi-major axis below MetOp-A) Backward: Drift opposite to the flight direction (semi-major axis above MetOp-A)
<i>No. of relative revolutions drifted</i>	0, 1, ...

With the purpose of defining an optimal strategy among the subset of accessible solutions a list of optimization criteria was defined by EUMETSAT-FD. The order of prioritization was stated as follows:

1. Fuel optimization. The positioning strategy shall be such that the required delta-V to implement it is minimized.
2. Time optimization. Among the subset of strategies which minimize the fuel, those ones minimizing the time to reach the final in-orbit target position for MetOp-B shall be selected.
3. Interference avoidance. The positioning strategy shall be such that the interference events with MetOp-A are minimized or, if possible, avoided.

4. Launch window analysis

The design of the positioning strategy had to account for a variable launch date. A non-fixed launch date translates into different initial positions of MetOp-B with respect to MetOp-A. This results in a set of different initial conditions for the phasing that had to be analysed in dedicated scenarios.

Since the LTDN to be achieved at injection is fixed there was a single launch opportunity per day determined by the solar local time of the launch site. Assuming that the ascending trajectory remains constant, the PSO of MetOp-B at separation was the same regardless of the launch date, whereas the position of MetOp-A at that epoch did depend on the launch date. Since the repeat pattern of the reference orbit is 412 revolutions in 29 days, the PSO of MetOp-A increases by 74.482 deg from one day to the next evaluated at the same solar time. This means that the relative PSO of MetOp-B at injection with respect to MetOp-A decreases by 74.482 deg from one day to the next. Therefore, 29 different cyclical initial relative PSOs arise depending on the launch date.

5. IP positioning. Reference ground track acquisition

The in-plane positioning of MetOp-B aimed at selecting the semi-major axis during the drift phase, a_{drift} , such that any of the two targets (A or B) was reached within the established positioning window. The selected approach had to meet the prioritized criteria mentioned in section 3.

Let a_{inj} be the mean semi-major axis at separation and a_{ref} the mean semi-major axis of the reference orbit. As mentioned in Tab. 2 a_{ref} is 16 km greater than a_{inj} . Neglecting second order effects, which are not relevant for the strategy design, it can be easily noticed that those strategies having a_{drift} between a_{inj} and a_{ref} , have the same delta-V consumption. Strategies of this kind have the lowest attainable delta-V for the in-plane positioning, which is the necessary one to overcome the semi-major axis difference from injection to the reference. An additional amount of fuel consumption is needed in strategies in which the semi-major axis is raised above the reference or lowered below the injection one. These strategies are needed in scenarios in which a backward drift is implemented or a faster drift is needed than the one imposed by a_{inj} , respectively.

The in-plane positioning scenarios were determined by the relative PSO of MetOp-B with respect to MetOp-A at the moment of the IP manoeuvre execution. A dedicated strategy was associated to each scenario. It can be inferred that the transitions of the relative PSO regions were a function only of semi-major axis dispersion at injection. The different scenarios are described hereinafter and depicted in Fig. 2.

- **Scenario A:** At least one of the targets is reached within a time span from 5 to 14 days after HO, with $a_{\text{drift}} = a_{\text{inj}}$. Within this scenario no IP correction is executed during LEOP. Any of the two targets (if available) may be selected.
 - Thresholds: **A1:** Target B is reached 5 days after HO.
A2: Target A is reached 14 days after HO.
- **Scenario B:** Target B is reached before 5 days after HO under the injection conditions, and target A has not been reached at the IP manoeuvre execution epoch. In this scenario the semi-major axis is changed so that the selected target is reached in 5 days, with $a_{\text{inj}} < a_{\text{drift}} < a_{\text{ref}}$. Both targets may be selected, the final decision depending on the target which simplifies the operations and minimizes risks.
 - Thresholds: **B1:** Equivalent to A1.
B2: Target A is reached at the IP manoeuvre execution epoch.
- **Scenario C:** Both targets are reached later than 14 days after HO at a_{inj} . In this scenario either a_{drift} has to be lowered below a_{inj} to increase the drift rate or raised above a_{ref} to implement a backward drift. The threshold defining the PSO where both drifting directions require the same delta-V is also computed (C2), which divides the scenario in two sub-scenarios. If a forward strategy is implemented, target A shall be targeted 14 days after HO; for a backward strategy target B shall be targeted 14 days after HO. The strategy to follow exactly at (or close to) C2 is a backward drift towards target B to avoid interferences with MetOp-A.
 - Thresholds: **C1:** Equivalent to A2
C2: PSO in which the cost of lowering the semi-major axis and reaching target A in 14 days after HO is the same as the one to drift backwards to target B in 14 days after HO.
C3: Target B is reached at the IP manoeuvre execution epoch.
- **Scenario D:** MetOp-B is located between both targets at the IP manoeuvre execution epoch. This scenario is a degradation of Scenario B. Target B shall be targeted unless the risk to miss the target due to manoeuvre underperformances is high, in which case a backward positioning towards target A shall be implemented.
 - Thresholds: **D1:** Equivalent to B2
D2: Equivalent to C3

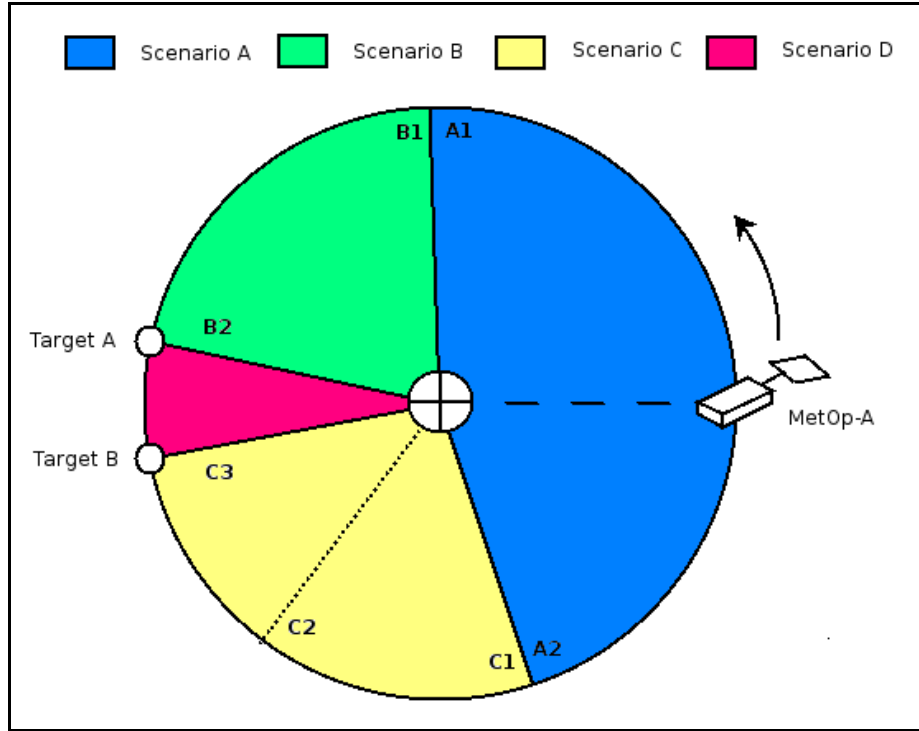


Figure 2. Scenarios for the in-plane positioning problem.

Table 4. Transitions of scenario regions determined by the relative PSO of MetOp-B with respect to MetOp-A at the time of the IP execution.

		Thresholds referred to IP execution epoch [deg]					Thresholds referred to separation [deg]				
		A1 = B1	B2 = D1	C3 = D2	C2	C1 = A2	A1 = B1	B2 = D1	C3 = D2	C2	C1 = A2
SMA [km] with respect to reference	-28	23.74	173.79	186.21	144.06	101.55	306.40	96.46	108.87	66.73	24.21
	-24	47.05	173.79	186.21	174.93	163.56	340.81	107.55	119.96	108.69	97.31
	-20	70.32	173.79	186.21	205.77	225.48	15.16	118.63	131.04	150.61	170.31
	-16	93.56	173.79	186.21	236.59	287.31	49.46	129.69	142.11	192.49	243.21
	-12	116.77	173.79	186.21	267.39	349.06	83.72	140.74	153.16	234.34	316.01
	-8	139.95	173.79	186.21	298.17	50.72	117.93	151.77	164.19	276.15	28.70
	-4	163.09	173.79	186.21	328.92	112.30	152.09	162.79	175.20	317.92	101.30

6. OOP correction and control of the LTDN

The OOP strategy to be implemented was conceptually very simple. If the injection state was leading to a violation of the upper bound of the control band (i.e. 9:30 + 120 sec) the inclination had to be decreased, targeting an optimal LTDN cycle. On the other hand, no inclination correction was necessary if the injection state implied a violation of the lower bound of the control band (i.e. 9:30 – 120 sec.) as long as no violation was taking place in the first 45 days after HO (HO conditions, section 3).

The real complexity of the OOP strategy laid on performing an exhaustive analysis to

demonstrate whether the HO conditions could be met for all possible injection cases. In particular, this analysis should determine which injections scenarios required and extension of the LEOP. The high complexity of the problem arose from:

- The large number of variables the LTDN evolution depended on
- The large dispersion in inclination that had to be taken as assumption for the analysis
- The limitations imposed by the LEOP operations schedule and the AOCS: by implementing only one OOP the maximum inclination correction was about 3 times lower than the 3-sigma dispersion provided by Soyouz.

The problem was tackled by the OD&C team at ESOC by means of the generation of the so-called drift-inclination diagrams (Fig. 6). In this type of diagrams the locus of points violating the LTDN control deadband in a particular time period was represented as a function of the inclination and the semi-major axis during the drift phase. The generation and interpretation of these diagrams is explained hereinafter.

6.1. Modeling of the LTDN evolution

Let λ be the difference between the actual LTDN of MetOp-B and the LTDN of the reference orbit. The evolution of λ from separation up to a given time t can be expressed as a function of the following variables:

- Initial offset of the function, λ_0 . Nominal injection is targeted at -70 s, with a 3-sigma dispersion of 26.3 s.
- Initial semi-major axis, a_0 . Nominal injection is targeted at 16 km below the reference, with a 3-sigma dispersion of 12 km.
- Initial inclination of the orbit plane, i_0 . Nominal injection is targeted at 35 mdeg above the reference, with a 3-sigma dispersion of 120 mdeg.
- Semi-major axis during the drift phase, a_{drift} , which is a function of the in-plane positioning strategy.
- Length of the drift phase, t_{drift} , which is a function of the in-plane position strategy, ranging from 5 to 14 days.
- Semi-major axis after the drift-stop manoeuvre. This variable will be controlled around the reference semi-major axis throughout the mission. The effect on λ of the small variation of this variable due to air drag and orbit maintenance manoeuvres can be neglected, and therefore be considered as a constant, a_{ref} .
- Inclination at the end of the LEOP after the execution of the OOP manoeuvre, i_3 , where 3 stands for the 3rd day of mission. Note that the absolute value of $i_3 - i_0$ is bounded by the maximum inclination change attainable, 50.8 mdeg.
- Time, t

$$\lambda = \lambda(\lambda_0, a_0, i_0, a_{drift}, t_{drift}, a_{ref}, i_3, t) \quad (1)$$

In Fig. 3 and Fig. 4 the behaviour of the previous function has been depicted for a particular set of input variables. After the execution of the drift-stop manoeuvre a quasi-parabolic behaviour of the function can be observed, due to the natural decrease of the inclination. However, the fact that during the drift phase the difference between semi-major axis the reference one is of the

order of kilometers leads to an almost linear behaviour of λ in time. This is because the characteristic time to notice parabolic effects under the conditions underwent in the drift phase is much larger than the length of the drift phase.

The first assumption taken was intended to simplify the dependency of λ with respect to a_0 and i_0 . Although the dispersions of a and i from their nominal values are quite large in terms of the necessary manoeuvres to correct for them, their short-term effect on the LTDN drift is relatively small. As a matter of fact, considering a 3-day long LEOP and 3-sigma dispersion values for a and i (both affecting the LTDN in the same direction), the value of λ at the end of the LEOP (λ_3) would differ by 14 seconds from the λ_3 corresponding to a nominal injection. This figure is of the same order of magnitude as the dispersion of the LTDN at injection (26.4 seconds 3-sigma dispersion). Thus, the initial conditions for λ can be transferred to the end of the LEOP removing the dependency from λ upon a_0 and i_0 and substituting λ_0 by λ_3 in Eq. 1, being the nominal value of $\lambda_3 = -61.616$ seconds.

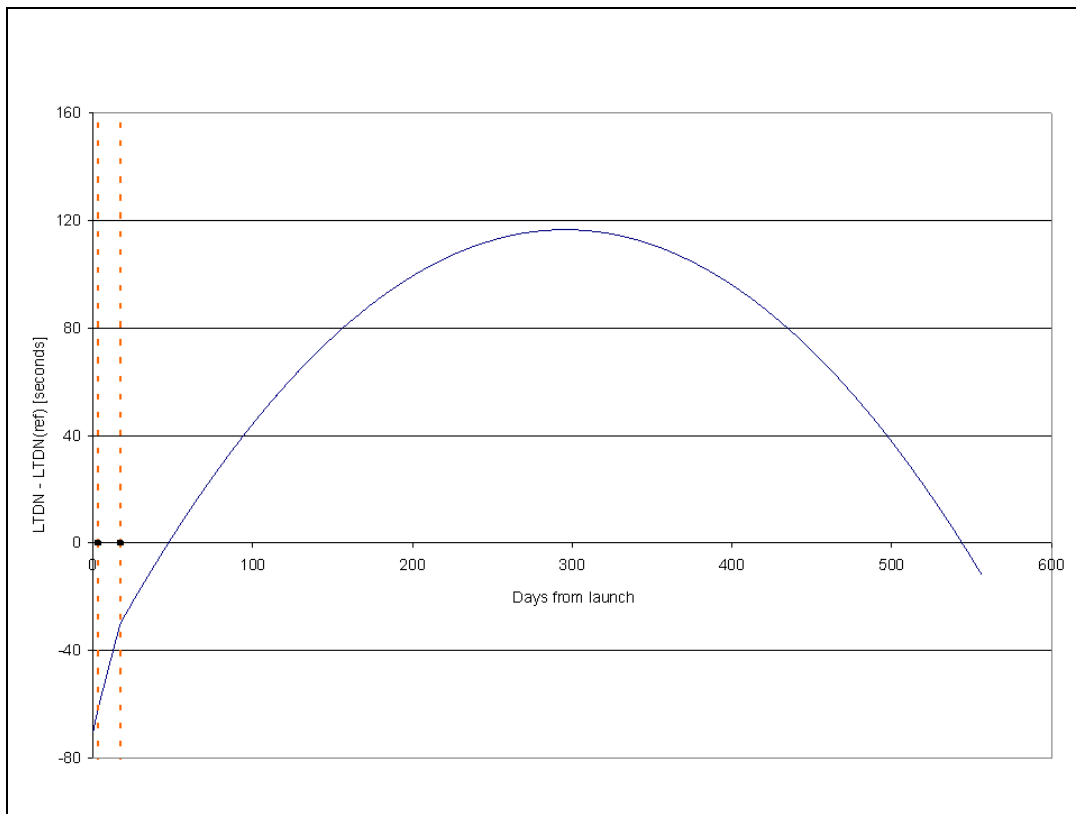


Figure 3. LTDN deviation using analytical models.

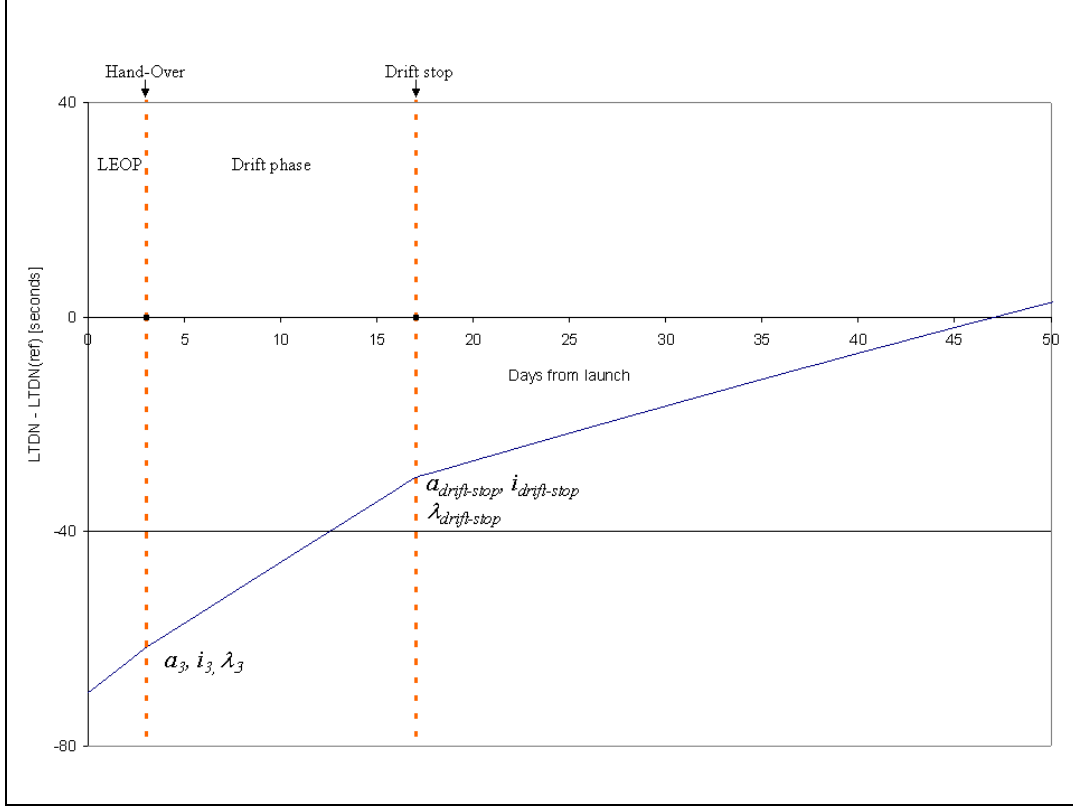


Figure 4. LTDN deviation using analytical models. Detail of the first days of mission.

The evolution of λ during the drift phase has been modeled assuming a linear behaviour in time, and by linearizing the dependencies upon the semi-major axis and the inclination, as it can be seen in the following equation.

$$\lambda_{drift-stop} = \lambda_3 + \lambda_a \Delta a \cdot t_{drift} + \lambda_i \Delta i \cdot t_{drift} \quad (2)$$

Where Δa and Δi are respectively the deviations of the semi-major axis and the inclination with respect to the reference during the drift phase. On the other hand λ_a and λ_i are the first order partial derivatives of λ with respect to the semi-major axis and the inclination respectively, evaluated at the reference orbit. They can be expressed as follows:

$$\lambda_a = \left(-\frac{7}{2}\right) \left(-\frac{3}{2}\right) J_2 \sqrt{\frac{\mu}{a_{ref}^3}} \left(\frac{R_{eq}}{a_{ref}}\right)^2 \frac{\cos i_{ref}}{a_{ref}} \quad (3)$$

$$\lambda_i = -\left(-\frac{3}{2}\right) J_2 \sqrt{\frac{\mu}{a_{ref}^3}} \left(\frac{R_{eq}}{a_{ref}}\right)^2 \sin i_{ref} \quad (4)$$

Being μ , R_{eq} and J_2 the gravitational parameter of the Earth, the equatorial radius of the Earth and the second order coefficient of the expansion of the Earth's potential in spherical harmonics. a_{ref} and i_{ref} are respectively the semi-major axis and the inclination of the reference orbit.

The behaviour of λ after the drift stop manoeuvre can be modeled as follows:

$$\lambda = \lambda_{drift-stop} + \int_{t_{drift-stop}}^t (\dot{\Omega} - \dot{\Omega}_{ref}) \cdot dt \quad (5)$$

Where $\dot{\Omega}$ represents the drift of the line of nodes and can be expressed as a function of the semi-major axis and the inclination, neglecting second order effects; $\lambda_{drift-stop}$ represents the value of λ at the time of the drift-stop manoeuvre.

Assuming the natural evolution of the inclination as a linear decrease of this parameter against time, the function λ can be expressed as follows (Ref. 2):

$$\lambda = A_0 + A_1(t' - t_{drift-stop}) + A_2(t' - t_{drift-stop})^2 \quad (6)$$

$$A_0 = \lambda_{drift-stop} \quad (7)$$

$$A_1 = -\dot{\Omega}_{ref} \operatorname{tg}(i_{drift-stop}) \Delta i \quad (8)$$

$$A_2 = -\frac{1}{2} \Omega_{ref} \operatorname{tg}(i_{drift-stop}) K_i \quad (9)$$

$$t' = t - t_{drift} \quad (10)$$

The time variable, t' , can be redefined as shown in Eq. 10 so that times are measured from HO. Nevertheless, one has to note that Eq. 6 is only valid for times greater or equal to $t_{drift-stop}$

The parameter introduced in Eq. 9, K_i represents the first derivative of the inclination with respect to time. The value of K_i is not constant. A seasonal variation of this parameter can be observed along the year as depicted in Fig. 5. In order to accurately model the behaviour of λ special care has to be taken in the selection of the time interval to average K_i . The best results were obtained by taking average intervals from 0.5 to 1 LTDN cycles (i.e. 9 – 18 months) from the launch date. It can be noticed that injection cases with a high dispersion in inclination, leading to an early exit of the LTDN control threshold, are also properly modeled by averaging K_i in a long time span, since the evolution of λ in those cases is dominated by the linear term of Eq. 3, A_1 . The value of K_i that was eventually selected to support the MetOp-B LEOP in September 2012 was -0.16 mdeg/day.

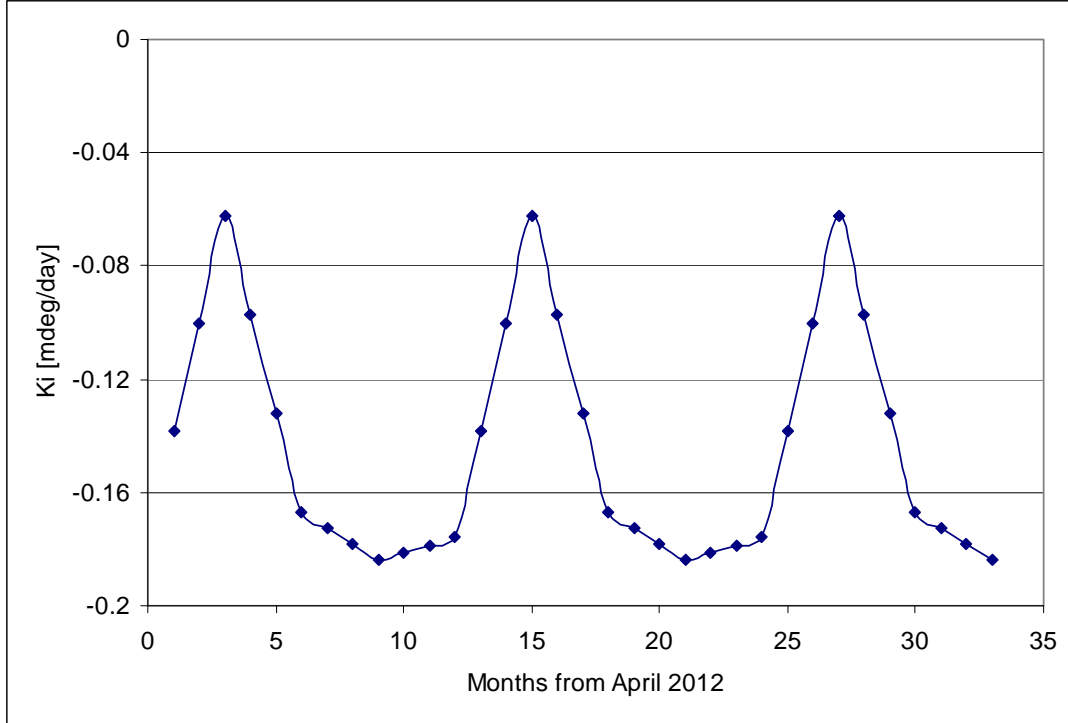


Figure 5. Seasonal variation of Ki.

Considering all the above assumptions, the evolution of the LTDN has been modeled as an initial value at HO, λ_3 ; a linear evolution in time given by Eq. 2; and a parabolic behaviour after the drift stop manoeuvre given by Eq. 6. The performances of this analytical model have been cross-checked against numerical propagations using NAPEOS (ESA software), giving satisfactory results. On the other hand, it can be noticed that the dependency of λ has been considerably reduced, as it is shown in Eq. 11, which allows the graphical depiction of the drift-inclination diagrams.

$$\lambda = \lambda(i_3, a_{drift}, \lambda_3, t_{drift}, t) \quad (11)$$

The generation of the drift-inclination diagrams consists of the representation in the (i_3, a_{drift}) plane of the curves given by the implicit equations which result of setting λ to the thresholds of the control band (± 120 seconds) for discrete values of t , and considering λ_3 and t_{drift} constant. Such curves represent the locus of points in which the control deadband for the LTDN is violated at selected discrete times. Of particular interest are the curves evaluated $t = 45$ days, which is the requirement stated in the HO conditions. The two curves shown in Eq. 12 represent upper and lower deadband violations 45 days after HO, taking the nominal value of λ_3 and a 14-days long drift phase.

$$\lambda(i_3, a_{drift}, \lambda_3 = -61.616 s, t_{drift} = 14 days, t = 45 days) = \pm 120 s \quad (12)$$

In Fig. 6 and 7 a set of such loci of points has been represented for deadband violations of 45, 90, 180 and 540 days after HO. The graphs were computed assuming a length of the drift phase of

5 and 14 days respectively, i.e. the lower and the upper bounds of the drift phase. The reference and the target inclination for the launcher are marked with vertical dashed lines in the graphs. On the right hand side of the graph the curves correspond to $\lambda = -120$ seconds and therefore represent violations of the lower threshold of the deadband, the opposite happens on the left hand side of the graph. The conditions in the central part of the graph represent LTDN cycles longer than 540 days, which is the nominal cycle length foreseen for MetOp-B in routine operations. All thick curves have been represented considering the nominal value of $\lambda_3 = -61.616$ seconds, the thin curves next to them were computed assuming a variation of this parameter of ± 10 seconds.

Given a state vector at injection the corresponding a_{drift} can be derived from the in-plane positioning strategy, and then the point (i_0, a_{drift}) can be located in the drift-inclination graph. By keeping a_{drift} constant a horizontal shift can be applied to this initial point up to the maximum inclination shift attainable with an OOP manoeuvre (i.e. 50.8 mdeg), reaching (i_3, a_{drift}) and providing a prediction of the LTDN cycle length. All this is possible since the dependency of λ with respect to i_0 was detached in the formulation described above.

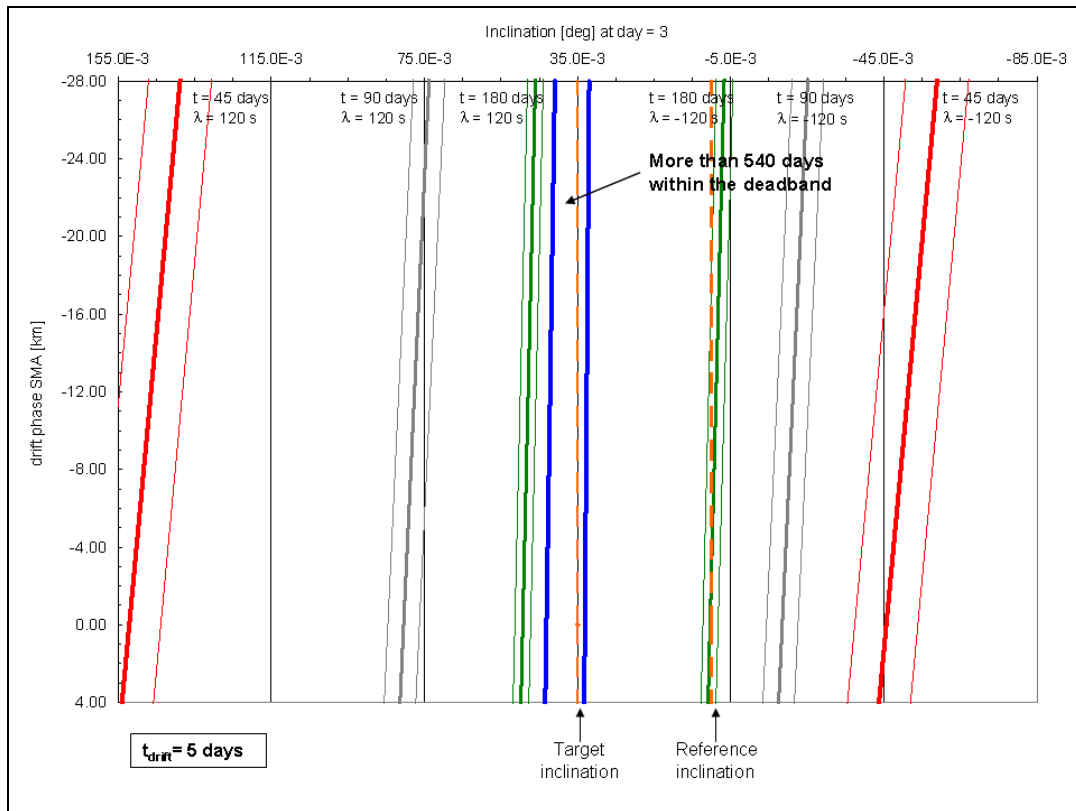


Figure 6. Drift-inclination diagram for a drift phase length of 5 days.

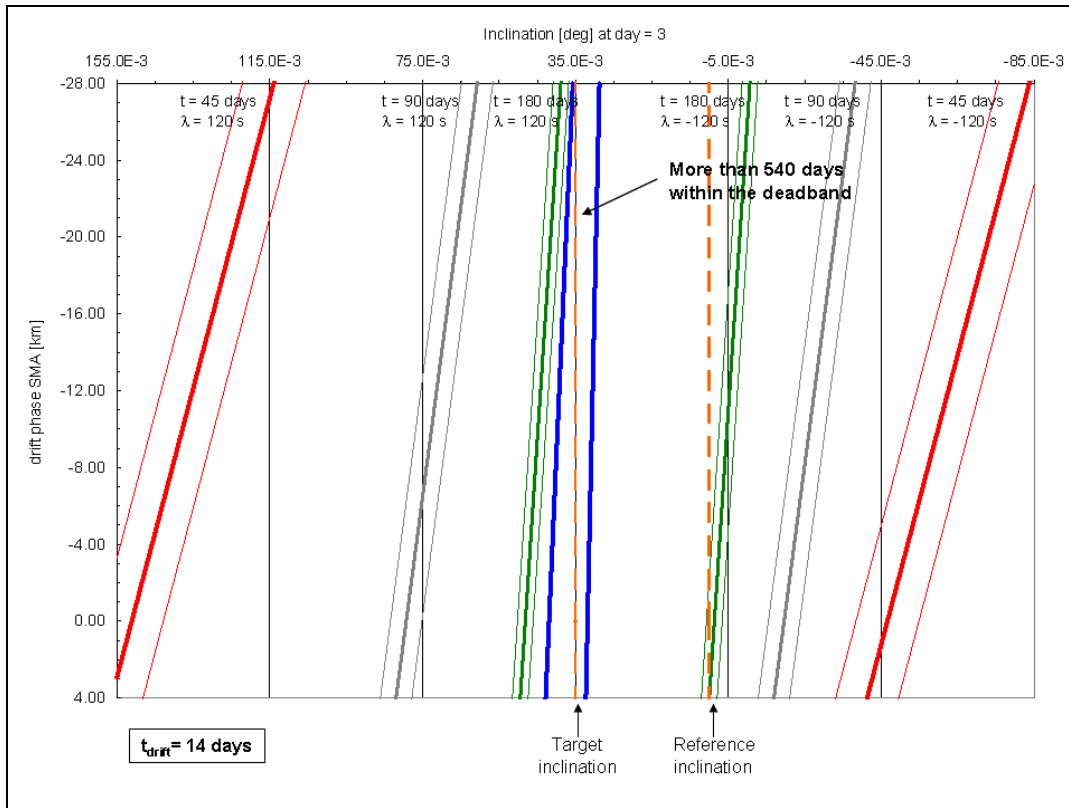


Figure 7. Drift-inclination diagram for a drift phase length of 14 days.

7. Simulation No. 1. Orbit scenario with large injection errors.

As part of the LEOP preparation several injection cases were prepared with the purpose of exercising the preparation and execution of the manoeuvring strategy. One of those cases was of particular interest to exemplify the decision-making process using the drift-inclination diagrams. The injection scenario in question was prepared for a launch on the 23rd of May 2012, which was the planned launch date before being delayed till the 17th of September. The simulated injection conditions were as follows:

- Injection semi-major axis 19.5 km below the reference (i.e. 4.5 km below the target)
- 3-sigma injection error in inclination. Let us consider both cases: 155 mdeg and -85 mdeg with respect to the reference.

On that particular launch day the semi-major axis mentioned above led to a PSO position of 180 deg relative to MetOp-A, that is exactly in the middle of both targets (Scenario D). Aiming at target B with a drift-phase length of 5 days would imply the execution of a large IP manoeuvre during LEOP (~9.35 m/s) and a smaller drift-stop manoeuvre (~0.74 m/s). By applying this strategy the semi-major axis during the drift phase would be approximately 1.43 km below the reference. The OOP manoeuvre would aim at correcting the inclination error as much as possible. Having a look at Fig. 6 and locating $a_{\text{drift}} = -1.43$ km one can observe that for an initial inclination offset of 155 mdeg and by applying the maximum attainable inclination correction (50.4 mdeg) the upper threshold of the deadband would be violated in a time interval longer than 45 days. However, if the initial inclination error was in the other direction

(-85 mdeg) by applying the maximum inclination correction the point would still lie very close to the 45-days line. Therefore, the HO requirements would be compromised.

An alternative to that strategy is to skip target B and select target A performing a whole revolution in PSO with respect to MetOp-A. In order to do this with a drift-phase length of 14 days the semi-major axis of MetOp-B has to be slightly lowered during LEOP (~1.85 m/s). In this case the semi-major axis during the drift phase would be approximately 23.2 km below the reference. It can be easily seen in Fig. 7 that, under these conditions, by applying the maximum correction in inclination to the initial -85 mdeg offset, the time interval until lower deadband violation would occur much later than 45 days, fulfilling the HO requirements.

8. LEOP Activities. Injection summary and selection of the positioning strategy

The first acquisition of MetOp-B took place at Kerguelen ground station, which reported a Time Offset Value (TOV) of 0.5 seconds (late). An increasing trend of the reported TOV was observed in subsequent passes, fact which was later on confirmed after the first Orbit Determination (OD). The estimated semi-major axis at injection was higher than the nominal one. An extract of the injection summary can be found in Tab. 5, which was produced after the first OD. These results were consolidated after the second OD, which introduced no significant changes to the state vector determined previously. At that stage, the preparation of the orbit positioning strategy could be started. The first step was to make an assessment of the phasing with respect to MetOp-A. A relative PSO equal to 48.271 deg, together with the semi-major axis offset of 3.076 km implied a scenario A from the in-plane positioning strategy cases. Without performing any IP manoeuvre target A was being reached in approximately 9.086 days, which was compliant with the HO requirements. Regarding the LTDN control, the very small offsets present in inclination and right ascension of ascending node led to an LTDN control cycle longer than 18 months without performing any OOP manoeuvre. Consequently, the HO requirements could have been met without any orbit correction.

The drawback of not executing any manoeuvre during the LEOP was the hand over of the MetOp-B operations with non-calibrated thrusters. This could have led to a bad performance of the drift-stop manoeuvre. In order to solve this problem the execution of a small IP manoeuvre was proposed by EUMETSAT representatives. The characteristics of the orbital change were as follows:

- Target A shall be aimed at 2012/09/27-12:30:00, which implies a delay in the arrival to the target of approximately 12 hours. Target B is kept as backup in case of contingency in the execution of the drift-stop manoeuvre.
- The IP manoeuvre shall be executed in a single burn, during the combined visibility of Hawaii, Alaska and Esrange, which allows the firing to be real time monitored.

Table 5. Injection summary.

Actual		Reference	Difference
X	2508.490348548	2508.184999991	0.305348557 km
Y	-819.076072212	-820.006999986	0.930927774 km
Z	-6692.165110231	-6688.690999966	-3.474110266 km
Xvel	5.038684721	5.039299999	-0.000615278 km/s
Yvel	-4.868509194	-4.869700000	0.001190806 km/s
Zvel	2.486052017	2.487699999	-0.001647982 km/s
S/M Axis	7175.651161676	7172.575216186	3.075945491 km
Eccentr.	0.002514011	0.002489697	0.000024314
Inclin.	98.695651115	98.693523910	0.002127204 deg
Asc.Node	319.094916475	319.092135880	0.002780595 deg
Arg.Per.	105.550067738	106.865218713	-1.315150974 deg
Tr.Anom.	184.211704271	182.908593974	1.303110297 deg

The IP manoeuvre was optimized to the following value:

Table 6. IP manoeuvre optimization.

Satellite 154			
2012/09/19-15:09:29.934 File generation time			
2012/09/19-15:05:14.139 Manoeuvre optimisation time			
Manoeuvre execution time	MODE	Size(m/s)	PSO(deg)
2012/09/20-06:53:00.000	INP GEO	0.53868	58.545

Although no eccentricity control was possible due to having a single fixed manoeuvring slot, the value of this orbital parameter was not compromised because of its small error at injection and the small size of the manoeuvre. Furthermore, the achievability of frozen eccentricity was granted by the bigger size of the drift-stop manoeuvre (approximately 6 m/s). More details on the manoeuvre execution and calibration can be found in a paper written by EUMETSAT for this same symposium [3].

9. References

- [1] K. Merz, M. A. Martín Serrano, D. Kuijper, M.A. García Matatoros. “The Metop-A orbit acquisition strategy and its LEOP operational experience” Proceedings 20th International Symposium on Space Flight Dynamics – 20th ISSFD. Annapolis, MD, USA, 2007
- [2] David A. Vallado. “Fundamentals of Astrodynamics and Applications” ISBN 0-7923-6903-3
- [3] P. Righetti, F. Sancho, T. Paulino. “Metop-B orbit acquisition operations; preparation and execution” Proceedings 23th International Symposium on Space Flight Dynamics – 23th ISSFD. Pasadena, California, USA, 2012.